JACS
JOURNAL OF THE AMERICAN CHEMICAL SOCIETY

Communication

pubs.acs.org/JACS

# Exploiting Noncovalently Conformational Locking as a Design Strategy for High Performance Fused-Ring Electron Acceptor Used in Polymer Solar Cells

Yahui Liu,[†,‡] Zhe Zhang,[†,‡] Shiyu Feng,[†] Miao Li,[†] Liangliang Wu,[†] Ran Hou,[†] Xinjun Xu,[*,†] Xuebo Chen,[†] and Zhishan Bo[*,†]

[†]Key Laboratory of Energy Conversion and Storage Materials, College of Chemistry, Key Laboratory of Theoretical and Computational Photochemistry, Ministry of Education, Beijing Normal University, Beijing 100875, P. R. China

Supporting Information

**ABSTRACT:** We have developed a kind of novel fused-ring small molecular acceptor, whose planar conformation can be locked by intramolecular noncovalent interaction. The formation of planar supramolecular fused-ring structure by conformation locking can effectively broaden its absorption spectrum, enhance the electron mobility, and reduce the nonradiative energy loss. Polymer solar cells (PSCs) based on this acceptor afforded a power conversion efficiency (PCE) of 9.6%. In contrast, PSCs based on similar acceptor, which cannot form a flat conformation, only gave a PCE of 2.3%. Such design strategy, which can make the synthesis of small molecular acceptor much easier, will be promising in developing a new acceptor for high efficiency polymer solar cells.

In recent years, fused-ring electron acceptors (FREAs) for use in polymer solar cells (PSCs) have received extensive attention due to their tunable energy levels and extended light absorption.[1,2] Such planar fused aromatic ring structure can facilitate $\pi$-electron delocalization, benefiting the decrease of energy band gap, the extension of light absorption, and the improvement in $\pi-\pi$ stacking among molecules. Currently, FREAs based on 4,9-dihydro-s-indaceno[1,2-*b*:5,6-*b*′]-dithiophene (IDT), 6,12-dihydroindeno[1,2-*b*]fluorene (IDF), and 6,12-dihydro-dithieno[2,3-*d*:2′,3′-*d*′]-s-indaceno[1,2-*b*:5,6-*b*′]dithiophene (IDTT) have demonstrated excellent photovoltaic performance with PCE higher than 8%.[3−12] However, the preparation of FREAs is usually tedious, which requires many synthesis and purification steps, especially for the large fused-ring structures.[13] Moreover, too strong $\pi-\pi$ stacking interactions arising from the high degree of coplanarity tend to decrease the solubility of materials in solutions, which in turn makes them easily aggregate, leading to a large phase separation in the solution-deposited donor:acceptor blend film.[14] Therefore, new molecular design strategy for small molecular acceptors is highly desired to solve the above problems.

Here, we developed a novel type of small molecular acceptor, we called it conformation locked fused-ring electron acceptor. We adopt noncovalently conformational locking as a molecular design strategy to endow acceptor molecules with a good planarity in solid state together with a good solubility in solutions. With such a molecular design, the coplanarity between neighboring aromatic rings, which are connected by a single bond, can be maintained through a locked conformation in the solid state via intramolecular noncovalent interactions (such as O···H, S···O, etc.) between the adjacent aromatic rings. While in solutions, the noncovalent interactions are not strong enough to lock the coplanar conformation, so distortion between neighboring aromatic rings is enabled and the solubility is improved. More importantly, as the realization of coplanarity between aromatic rings through noncovalent interactions is much more facile than that through a covalent bridge in fused-ring structures, the synthesis procedure will be largely simplified. In 2013, through theoretical computations Jackson et al. noted that nontraditional hydrogen-bonding interactions, oxygen−hydrogen (CH···O) and nitrogen−hydrogen (CH···N), could induce conformational control and enhance the planarity along a polymer backbone at room temperature.[15] Experimentally, polymer backbones with noncovalently conformational locking were used in the design of polymers for field-effect transistors and polymer donor materials for photovoltaics, and these polymers tend to show good flatness and high mobilities.[16−20] However, currently, utilization of noncovalent interactions to lock the molecular conformation of small molecular acceptors has not been reported yet. In addition, the relationship between device performance and chemical geometry structure in designing small molecular acceptors is still unclear.

In this communication, we designed and synthesized two small molecular acceptors (**IDT-BC6** and **IDT-BOC6**) with IDT as a central core unit, bis(alkoxy)-substituted or dialkyl-substituted benzene ring as conformational control units, and cyano-indanones as end-capping units. It is worth noting that these two compounds can be easily synthesized in two steps. We have carefully studied the differences of alkyl and alkoxy substituted acceptors in UV absorptions, energy levels, DFT calculations, and device performances. As expected, the acceptor (**IDT-BOC6**) with noncovalently conformational locking exhibited a quite good planarity in the solid state. In addition, good planarity and rigidity in **IDT-BOC6** endow it with a higher fluorescence quantum yield relative to **IDT-BC6**, which means the energy loss arising from nonradiative recombination is reduced. As a result, an increased open-circuit voltage ($V_{oc}$) can be expected.[3] When used in PSCs, **IDT-BOC6** demonstrated a maximum power

**Received:** January 17, 2017
**Published:** February 22, 2017





DOI: 10.1021/jacs.7b00566
J. Am. Chem. Soc. 2017, 139, 3356−3359

conversion efficiency of 9.6% and a very high $V_{oc}$ of 1.01 V, which is among the highest $V_{oc}$ values reported for high-efficiency nonfullerene PSCs.[3,4,7,21]

The synthetic route of **IDT-BC6** and **IDT-BOC6** is shown in Scheme 1. The aldehyde intermediates **IDT-B6** and **IDT-BO6**

**Scheme 1**[a]

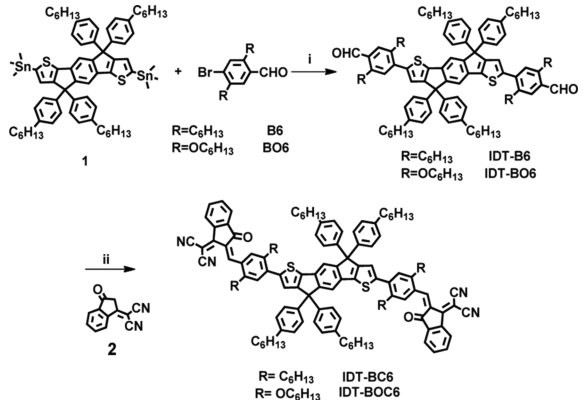


[a]Reagents and conditions: (i) $Pd(PPh_3)_4$, toluene, reflux; (ii) pyridine, $CHCl_3$, reflux.

were prepared in yields of 90% and 88% by Stille coupling of **1** with **B6** and **BO6**,[22,23] respectively, using $Pd(PPh_3)_4$ as the catalyst precursor. The target molecules **IDT-BC6** and **IDT-BOC6** were obtained in yields of 62% and 58%, respectively, by end-capping with **2**. These two compounds exhibit good solubility in common solvents such as dichloromethane, chloroform, and *o*-dichlorobenzene (DCB).

UV−vis absorption properties of **PBDB-T**,[11] **IDT-BOC6**, and **IDT-BC6** as thin films were investigated, and their spectra are shown in Figure 1. They exhibit two absorption bands, the one at

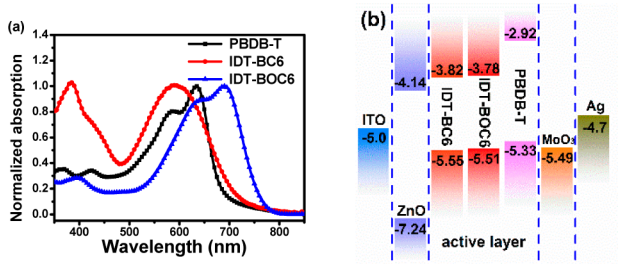


**Figure 1.** (a) Absorption spectra of **PBDB-T**, **IDT-BC6**, and **IDT-BOC6** in thin films and (b) energy band diagram.

shorter wavelength corresponds to the $\pi-\pi^*$ transition, and the other one at longer wavelength originates from the intramolecular charge transfer (ICT) transition.[24] Specifically, **IDT-BC6** exhibits a broad and featureless absorption band in the range of 450 to 750 nm with a peak at 592 nm; whereas **IDT-BOC6** displays a well-resolved and red-shifted absorption band ranging from 500 to 800 nm with two peaks at 636 and 688 nm, indicating the effective conjugation length is extended after replacing alkyl side chain with alkoxy side chain. Moreover, such a large red shift together with a significant decreasing of the $\pi-\pi^*$ transition band (~390 nm) intensity indicate that the delocalization of $\pi$-electrons is enhanced,[18,25] which is probably due to the improvement in the coplanarity of **IDT-BOC6** (vide infra). It is worth noting that **IDT-BOC6** exhibits complementary absorption with PBDB-T. Thermogravimetric analysis (TGA) indicates that **IDT-BC6** and **IDT-BOC6** have a good thermal stability with decomposition temperatures (5% weight loss) up to 333 and 338 °C (Figure S2), respectively, under nitrogen protection. There is no obvious glass transition observed by differential scanning calorimetry (DSC) measurement in the range of 80 to 300 °C (see Supporting Information). The optical bandgap of **IDT-BC6** was calculated to be 1.75 eV according to the equation: $E_{g,opt} = 1240/\lambda_{onset}$, which is slightly higher than that of **IDT-BOC6** (1.63 eV). The electrochemical properties of these two acceptors were studied by cyclic voltammetry (CV). As shown in Figure S5, according to the equation $E_{HOMO/LUMO} = -e(E_{onset,ox/red} + 4.71\ eV)$,[26] the highest occupied molecular orbital (HOMO) and the lowest unoccupied molecular orbital (LUMO) energy levels were calculated to be −5.55 and −3.82 eV for **IDT-BC6** and −5.51 and 3.78 eV for **IDT-BOC6**, respectively. The detailed data are summarized in Table 1. The energy levels of these two acceptors and other materials used for fabricating photovoltaic devices are also shown in Figure 1b.

**Table 1. Physical, Electronic, and Optical Properties of IDT-BC6 and IDT-BOC6**

| NF-SM | $\lambda_{max}$ (nm) film | $E_g$ (eV) | HOMO (eV) | LUMO (eV) |
|---|---|---|---|---|
| IDT-BC6 | 592 | 1.75 | −5.55 | −3.82 |
| IDT-BOC6 | 636, 688 | 1.63 | −5.51 | −3.78 |

Density functional theory (DFT) calculations at the B3LYP/6-31G(d) level were also performed to investigate the chemical geometry of **IDT-BC6** and **IDT-BOC6** with simplified side chains as shown in Figure 2. The dihedral angles between the 1,4-phenylene unit in the main chain and its neighboring units exhibit a big difference for **IDT-BC6** and **IDT-BOC6**. The two dihedral angles for the simplified **IDT-BC6** molecule are 47° and 36°; whereas the two dihedral angles are reduced to 9° and 1° for

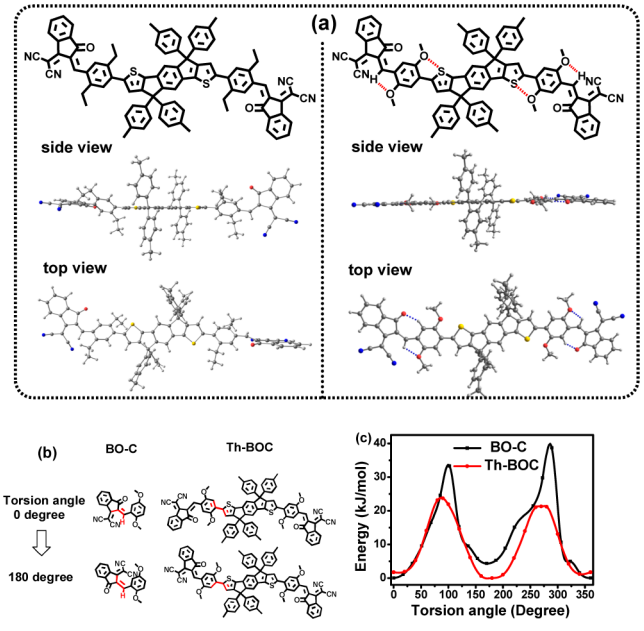


**Figure 2.** (a) Simulated molecular geometries obtained by DFT calculations for simplified molecules of **IDT-BC6** and **IDT-BOC6**. (b) Possible rotamers (BO-C and Th-BOC) in **IDT-BOC6** and (c) potential energy surface scan of BO-C and Th-BOC.



DOI: 10.1021/jacs.7b00566
J. Am. Chem. Soc. 2017, 139, 3356−3359

the simplified **IDT-BOC6** molecule. To further understand such a huge difference for dihedral angles, relaxed potential surface energy scans of possible rotamers in **IDT-BOC6** have been carefully studied. There are two potential rotamers in the backbone of **IDT-BOC6**, which are called BO-C and Th-BOC. First, the BO-C rotamer could be locked-up in an energy preferred conformation of 0° with O···H intramolecular interactions. Second, given the preferred conformation of the BO-C rotamer, the Th-BOC rotamer was further studied. Figure 2b,c shows that the Th-BOC rotamer could be locked-up in a 180° conformation at the lowest energy state via H···O and S···O intramolecular interactions. Such phenomenon is called non-covalently conformational locking.[17,18] Such a conformational locking leads to delocalized LUMO level, and the resulting planar geometry is beneficial to $\pi-\pi$ stacking, which is advantageous for charge transport.

Bulk-heterojunction polymer solar cells were fabricated with an inverted device structure of ITO/ZnO (30 nm)/active layer (100 nm)/$MoO_3$ (80 Å)/Ag (100 nm). The ZnO layer was prepared as pervious reported,[27] and the active layer consisted of PBDB-T and **IDT-BC6** or **IDT-BOC6**. A range of conditions such as polymer concentrations, solvents, active layer composition (weight ratios), spin coating rates, and additives were systematically investigated. The optimized donor (**PBDB-T**) to acceptor (**IDT-BC6** or **IDT-BOC6**) ratio is 1:1 (weight by weight, w/w), and the thickness of active layer was about 100 nm (Table S3) at a spin coating rate of 1750 r/min with dilute *o*-dichlorobenzene solutions (polymer concentration: 4 mg/mL). The optimizing process is described in the Supporting Information. The optimized device parameters are shown in Table 2. The current density−voltage ($J-V$) curves and external

**Table 2. Photovoltaic parameter of PBDB-T:IDT-B(O)C6 Based Optimized Devices**

| device | DIO | $V_{oc}$ (V) | $J_{sc}$ (mA/cm$^2$) | FF (%) | PCE (%) |
|---|---|---|---|---|---|
| IDT-BC6 | | 0.92 | 5.63 (5.36)[a] | 44 | 2.3 (2.17)[b] |
| IDT-BOC6 | | 1.01 | 15.35 (14.61)[a] | 55 | 8.49 (8.41)[b] |
| | 1% | 1.01 | 17.52 (16.89)[a] | 54 | 9.60 (9.43)[b] |

[a]Calculated by EQE measurement. [b]Average PCE of 10 devices.

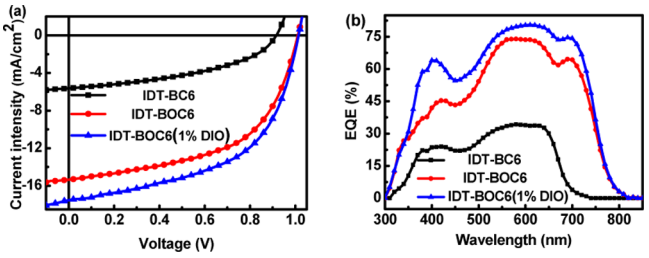


**Figure 3.** (a) $J-V$ and (b) EQE curves of **PBDB-T:IDT-B(O)C6** based devices.

quantum efficiency (EQE) curves are displayed in Figure 3. **IDT-BC6** based devices gave a PCE of 2.28% with a $V_{oc}$ of 0.92 V, a short circuit current ($J_{sc}$) of 5.63 mA/cm$^{-2}$, and a fill factor (FF) of 44.2%. In comparison, **IDT-BOC6** based devices exhibited a PCE of 8.49% with a higher $V_{oc}$ of 1.01 V, a $J_{sc}$ of 15.35 mA/cm$^{-2}$, and an FF of 54.7%. After the addition of 1% 1,8-diiodoctane (DIO), the PCE was further enhanced to 9.60% with a higher $J_{sc}$ value of 17.52 mA/cm$^{-2}$. It is worth noting that the $V_{oc}$ of **IDT-BOC6** based devices is 0.1 V higher than that of **IDT-BC6** based ones. Although **IDT-BOC6** has a higher LUMO energy level than **IDT-BC6**, the small difference (0.04 eV) between them is not enough to explain their relatively large $V_{oc}$ difference (~0.1 V). Since nonradiative recombination process in the active layer is a key factor to influence the voltage loss ($\Delta V$), we thus measured the absolute fluorescence quantum yields ($\eta_{FL}$) of **IDT-BC6** and **IDT-BOC6** films. An $\eta_{FL}$ value of 7.4% was obtained for **IDT-BOC6**, while that was only 2.0% for **IDT-BC6**, which is in accordance with the result reported in literature that compounds with a more planar and rigid molecular geometry demonstrate a higher $\eta_{FL}$ value.[28,29] This means energy loss (thus voltage loss) in solar cells through nonradiative recombination is smaller for **IDT-BOC6** than for **IDT-BC6**. Therefore, **IDT-BOC6** gives a higher $V_{oc}$ than **IDT-BC6**. The higher $J_{sc}$ in devices based on **IDT-BOC6** relative to **IDT-BC6** can be attributed to its broader phototo-to-current response (Figure 3b) and its more planar molecule geometry, which is beneficial for the $\pi-\pi^*$ stacking between molecules to get a higher carrier mobility.

In order to better understand the big difference between **IDT-BC6** and **IDT-BOC6** based devices, the morphology of blend films was investigated by atomic force microscope (AFM) in tapping mode and transmission electron microscope (TEM). As shown in Figure 4, thick fibrils of PBDB-T were formed in the

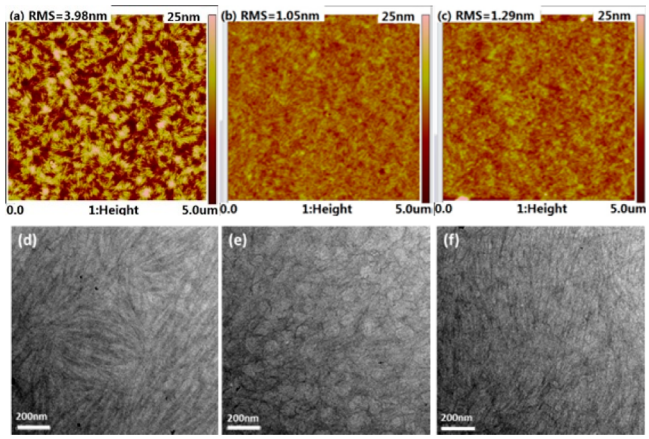


**Figure 4.** AFM images of (a) **PBDB-T:IDT-BC6** film; (b) **PBDB-T:IDT-BOC6** film; (c) **PBDB-T:IDT-BOC6** film spin coated with DCB (1% DIO) and TEM images of (d) **PBDB-T:IDT-BC6** film; (e) **PBDB-T:IDT-BOC6** film; and (f) **PBDB-T:IDT-BOC6** film spin coated with DCB (1% DIO).

spin-coated **PBDB-T:IDT-BC6** blend films, and the root mean squire (RMS) roughness is 3.98 nm, which is higher than **IDT-BOC6** based active layers (1.05 nm). As for **PBDB-T:IDT-BOC6** blend film (without DIO addition), coiled PBDB-T fibrils in a smaller diameter were observed. After the addition of DIO, the fibrils of **PBDB-T** tend to arrange more orderly than those without DIO addition. Appropriate phase separation scale of **IDT-BOC6** based active layer is beneficial to the exciton dissociation and charge transport in devices.

To further elucidate the influence of chemical structure of small molecular acceptors on the charge transportation properties of blend films, hole and electron mobilities were measured with a device structure of ITO/PEDOT:PSS (30 nm)/active layer (100 nm)/Au (100 nm) and FTO/active layer (100 nm)/Al (100 nm), respectively. As shown in Figure S1, the hole mobility and electron mobilities of **IDT-BC6** based devices were calculated to be 2.89 × 10$^{-6}$ and 1.38 × 10$^{-6}$ cm$^2$/(V s),


DOI: 10.1021/jacs.7b00566
J. Am. Chem. Soc. 2017, 139, 3356−3359

respectively. In contrast, **IDT-BOC6** based devices exhibit much higher hole and electron mobilities ($1.68 \times 10^{-4}$ and $1.98 \times 10^{-4}$ $cm^2/(V\,s)$, respectively). The higher carrier mobility in the active layer of **IDT-BOC6** relative to **IDT-BC6** can explain its higher $J_{sc}$ value in PSCs. We notice that the FF of **IDT-BOC6** is only 54%, which is not very high. The reason is not clear yet since FF can be affected by either device or bulk heterojunction features.[30] One possible explanation is that the buffer layer (ZnO) or the ZnO/organic interface still needs to be optimized. After 1% DIO added, the mobility was further enhanced about two times ($\mu_h$ = $5.31 \times 10^{-4}$ $cm^2/(V\,s)$; $\mu_e = 4.99 \times 10^{-4}$ $cm^2/(V\,s)$), which can explain the $J_{sc}$ increase from 15.35 to 17.52 $mA/cm^2$. The mobility result is quite consistent with photovoltaic parameters.

In summary, noncovalent intramolecular interactions were purposefully introduced to the design of large supramolecular fused-ring acceptors. Supramolecular interaction can lock the flat conformation of **IDT-BOC6** acceptor, which can significantly extend the effective conjugation and broaden the absorption spectrum. **IDT-BOC6** with locked conformation showed a higher quantum yield, which can effectively suppress the nonradiative energy loss and afford higher $V_{oc}$ for devices. Our results thus provide an effective strategy for the design of high-performance nonfullerene small molecular acceptors with low synthetic cost.

## ■ ASSOCIATED CONTENT

### Supporting Information

The Supporting Information is available free of charge on the ACS Publications website at DOI: 10.1021/jacs.7b00566.

Experimental details, spectral data of all compounds, DFT calculations, TGA, DSC, CV and SCLC measurements, XRD data, OPV fabrication and measurements (PDF)

## ■ AUTHOR INFORMATION


### Corresponding Authors

*xuxj@bnu.edu.cn

*zsbo@bnu.edu.cn

### ORCID

Xuebo Chen: 0000-0002-9814-9908

Zhishan Bo: 0000-0003-0126-7957


### Author Contributions

‡Y.L. and Z.Z. contributed equally to this work.

### Notes

The authors declare no competing financial interest.

## ■ ACKNOWLEDGMENTS

Financial support from the National Natural Science Foundation of China (91233205, 20774099, 21574013, and 51673028) and Program for Changjiang Scholars and Innovative Research Team in University is gratefully acknowledged.

## ■ REFERENCES


(1) Nielsen, C. B.; Holliday, S.; Chen, H. Y.; Cryer, S. J.; Mcculloch, I. *Acc. Chem. Res.* **2011**, *48*, 2803.

(2) Lin, Y.; Zhan, X. *Acc. Chem. Res.* **2015**, *49*, 175.

(3) Liu, J.; Chen, S.; Qian, D.; Gautam, B.; Yang, G.; Zhao, J.; Bergqvist, J.; Zhang, F.; Ma, W.; Ade, H.; Inganäs, O.; Gundogdu, K.; Gao, F.; Yan, H. *Nat. Energy* **2016**, *1*, 16089.

(4) Meng, D.; Fu, H.; Xiao, C.; Meng, X.; Winands, T.; Ma, W.; Wei, W.; Fan, B.; Huo, L.; Doltsinis, N. L.; Li, Y.; Sun, Y.; Wang, Z. *J. Am. Chem. Soc.* **2016**, *138*, 10184.

(5) Yao, H.; Chen, Y.; Qin, Y.; Yu, R.; Cui, Y.; Yang, B.; Li, S.; Zhang, K.; Hou, J. *Adv. Mater.* **2016**, *28*, 8283.

(6) Feng, L.; Zhou, Z.; Cheng, Z.; Vergote, T.; Fan, H.; Feng, L.; Zhu, X. *J. Am. Chem. Soc.* **2016**, *138*, 15523.

(7) Baran, D.; Ashraf, R. S.; Hanifi, D. A.; Abdelsamie, M.; Gasparini, N.; Röhr, J. A.; Holliday, S.; Wadsworth, A.; Lockett, S.; Neophytou, M.; Emmott, C. J. M.; Nelson, J.; Brabec, C. J.; Amassian, A.; Salleo, A.; Kirchartz, T.; Durrant, J. R.; McCulloch, I. *Nat. Mater.* **2017**, *16*, 363.

(8) Bin, H.; Zhang, Z. G.; Gao, L.; Chen, S.; Zhong, L.; Xue, L.; Yang, C.; Li, Y. *J. Am. Chem. Soc.* **2016**, *138*, 4657.

(9) Bin, H.; Gao, L.; Zhang, Z. G.; Yang, Y.; Zhang, Y.; Zhang, C.; Chen, S.; Xue, L.; Yang, C.; Xiao, M.; Li, Y. *Nat. Commun.* **2016**, *7*, 13651.

(10) Lu, H.; Zhang, J.; Chen, J.; Liu, Q.; Gong, X.; Feng, S.; Xu, X.; Ma, W.; Bo, Z. *Adv. Mater.* **2016**, *28*, 9559.

(11) Li, S.; Ye, L.; Zhao, W.; Zhang, S.; Mukherjee, S.; Ade, H.; Hou, J. *Adv. Mater.* **2016**, *28*, 9423.

(12) Yang, Y.; Zhang, Z.-G.; Bin, H.; Chen, S.; Gao, L.; Xue, L.; Yang, C.; Li, Y. *J. Am. Chem. Soc.* **2016**, *138*, 15011.

(13) Li, Y.; Liu, X.; Wu, F. P.; Zhou, Y.; Jiang, Z. Q.; Song, B.; Xia, Y.; Zhang, Z. G.; Gao, F.; Inganäs, O.; Li, Y.; Liao, L. *J. Mater. Chem. A* **2016**, *4*, 5890.

(14) Zhang, J.; Xie, S.; Zhang, X.; Lu, Z.; Xiao, H.; Li, C.; Li, G.; Xu, X.; Chen, X.; Bo, Z. *Chem. Commun.* **2017**, *53*, 537.

(15) Jackson, N. E.; Savoie, B. M.; Kohlstedt, K. L.; Olvera de la Cruz, M.; Schatz, G. C.; Chen, L. X.; Ratner, M. A. *J. Am. Chem. Soc.* **2013**, *135*, 10475.

(16) Qin, R.; Li, W.; Li, C.; Du, C.; Veit, C.; Schleiermacher, H. F.; Andersson, M.; Bo, Z.; Liu, Z.; Inganäs, O.; Wuerfel, U.; Zhang, F. *J. Am. Chem. Soc.* **2009**, *131*, 14612.

(17) Huang, H.; Chen, Z.; Ortiz, R. P.; Newman, C.; Usta, H.; Lou, S.; Youn, J.; Noh, Y.-Y.; Baeg, K.-J.; Chen, L. X.; Facchetti, A.; Marks, T. *J. Am. Chem. Soc.* **2012**, *134*, 10966.

(18) Uddin, M. A.; Lee, T. H.; Xu, S.; Song, Y. P.; Kim, T.; Song, S.; Nguyen, T. L.; Ko, S.; Hwang, S.; Jin, Y. K.; Han, Y. W. *Chem. Mater.* **2015**, *25*, 5997.

(19) Lei, T.; Xia, X.; Wang, J. Y.; Liu, C. J.; Pei, J. *J. Am. Chem. Soc.* **2014**, *136*, 2135.

(20) Lei, T.; Dou, J. H.; Cao, X. Y.; Wang, J. Y.; Pei, J. *J. Am. Chem. Soc.* **2013**, *135*, 12168.

(21) Baran, D.; Kirchartz, T.; Wheeler, S.; Dimitrov, S.; Abdelsamie, M.; Gorman, J.; Ashraf, R. S.; Holliday, S.; Wadsworth, A.; Gasparini, N.; Kaienburg, P.; Yan, H.; Amassian, A.; Brabec, C. J.; Durrant, J. R.; McCulloch, I. *Energy Environ. Sci.* **2016**, *9*, 3783.

(22) Tu, G.; Li, H.; Forster, M.; Heiderhoff, R.; Balk, L. J.; Scherf, U. *Macromolecules* **2006**, *39*, 4327−4331.

(23) Norris, B. N.; Zhang, S.; Campbell, C. M.; Auletta, J. T.; Calvomarzal, P.; Hutchison, G. R.; Meyer, T. Y. *Macromolecules* **2013**, *46*, 1384−1392.

(24) Liu, Q.; Li, C.; Jin, E.; Lu, Z.; Chen, Y.; Li, F.; Bo, Z. *ACS Appl. Mater. Interfaces* **2014**, *6*, 1601.

(25) Brabec, C. J.; Heeney, M.; McCulloch, I.; Nelson, J. *Chem. Soc. Rev.* **2011**, *40*, 1185.

(26) Jin, E.; Du, C.; Wang, M.; Li, W.; Li, C.; Wei, H.; Bo, Z. *Macromolecules* **2012**, *45*, 7843.

(27) Sun, Y.; Seo, J. H.; Takacs, C. J.; Seifter, J.; Heeger, A. J. *Adv. Mater.* **2011**, *23*, 1679.

(28) Nijegorodov, N. I.; Downey, W. S. *J. Phys. Chem.* **1994**, *98*, 5639.

(29) Nijegorodov, N.; Zvolinsky, V.; Luhanga, P. V. C. *J. Photochem. Photobiol., A* **2008**, *196*, 219.

(30) Jao, M.; Liao, H.; Su, W. *J. Mater. Chem. A* **2016**, *4*, 5784.




DOI: 10.1021/jacs.7b00566
*J. Am. Chem. Soc.* 2017, 139, 3356−3359